Kufa Journal of Engineering
Vol. 17, No. 3, July 2026, P.P. 584-600
Article history: Received 27 September 2025, last revised 23 December 2025, accepted 4 January 2026

INFLUENCE OF CRYSTAL GROWTH ON THE MECHANICAL PROPERTIES AND SURFACE ROUGHNESS OF LAS GLASS CERAMICS FOR DENTAL APPLICATIONS

Ayad saad abd al-karim[1]and Zaid G. A. Al-jlaihawi[2]

[1] University of Kufa, College of Engineering, Department of Mechanical Engineering, Najaf, Iraq.

[2] University of Kufa, College of Engineering, Department of Mechanical Engineering, Najaf, Iraq, Email:zaidgh.abdulkadhim@uokufa.edu.iq.

https://doi.org/10.30572/2018/KJE/170333

ABSTRACT

Glass-ceramics of the lithium aluminosilicate (LAS) system are widely employed in dentistry; yet optimizing their clinical performance requires specific control of heat treatment parameters. This study aims to investigate the impact of varied processing parameters on the resulting microstructure, mechanical properties, and surface roughness of these materials. The methodology involves systematic control of nucleation temperature (520°C) and crystallizations temperatures (750°C) and (900°C). Materials were micro-structurally characterized and investigated using X-ray diffraction (XRD) and Scanning Electron Microscopy (SEM); mechanically using Knoop hardness tests and ultrasound wave velocity (to obtain an elastic modulus; and physically using a surface roughness tester. XRD confirmed the presence of $LiAlSi_2O_6$ as the main phase and $Li_2Si_2O_5$ as a minor phase. Furthermore, the optimal heat treatment of glass-ceramics significantly increased the knoop hardness amounted to ~ 7.66±0.44GPa and the elastic modulus to ~ 96.35±0.50GPa. Surface roughness analysis also revealed a minimum (Ra) of 0.34±0.04μm for the specific heat treatment.

KEYWORDS

Glass-ceramics; Lithium aluminosilicate; Lithium disilicate; Crystallization; Crystal growth; Knoop hardness; Elastic modulus; Surfaces roughness.

1. INTRODUCTION

Biomaterials are designed for medical and dental applications are broadly classified based on their intended biological interaction and material type. Historically, materials fell into four general categories: metals such as titanium alloys for implants (Abd-Elaziem et al., 2024), polymers e.g. natural rubber (Abdulkadhim, 2014; Jweeg and Al-Jlaihawi, 2021), composites such as functionally graded materials (FGMs) (Al-hadrayi and Khaleel, 2025; Jasim and Abdulsamad, 2025) and ceramics such as glass-ceramics. On the other hand, these materials can be functionally classified the bioactive materials and the bioresorbable materials, based on their mechanism of interaction with the body's biological systems (El-Meliegy and Noort, 2012). In restorative dentistry, glass-ceramics are highly valued for their exceptional biocompatibility, wear resistance, and aesthetic properties, making an ideal choice for durable dental restorations (Pershin et al., 2018; Remote et al., 2019; Fu, Engqvist and Xia, 2020). The physical properties such as roughness surface and mechanical properties such as hardness and elastic modulus of materials rely significantly on their resulting microstructure (Fatlawi, Jármai and Kovács, 2021; Zainy et al., 2025). Glass-ceramics are advanced composite materials characterized by multiple crystalline phases uniformly distributed within a glassy matrix (W. Höland and G. H. Beall, 2012). They are synthesized by subjecting a base glass to a carefully controlled, multi-stage heat treatment, process (often termed "ceramming"), which precisely promotes the nucleation and subsequent growth of crystals (W. Höland and G. H. Beall, 2012; Zhou et al., 2022). This controlled crystallization ensures a fine and even dispersion of crystals throughout the material. While crystallization can approach completion a small portion of the original glass may distinctly remain as an amorphous structure, a phenomenon often associated with the impurity level of raw materials and the specific ceramic processing system (Deubener et al., 2018; Honma et al., 2022). Lithium Alumina Silicate (LAS) glass-ceramics are particularly noteworthy for their exceptional properties, including excellent chemical durability, low thermal expansion, bio-compatibility, appealing aesthetics, and high mechanical strength typically derived from the formation of two main crystalline phases $LiAlSi_2O_6$ and $Li_2Si_2O_5$ (Adolfsson and Shen, 2014; Kordatos, Abdulkadhim and Feteira, 2017). Previous studies have explored the crystallization kinetics and phase compositions of these systems. (Holand et al., 2006) studied the crystallization analysis, the composition of the primary phase in a complex lithium disilicate ceramics of system SiO_2-Li_2O-Al_2O_3-k_2O-ZrO_2-P_2O_5 identifying a glass transition temperature range ~ 480°C. The authors (Laczka et al., 2014) investigated the ternary phase diagram of the Li_2O-Al_2O_3-SiO_2-k_2O system. They found that the glass transition temperature range 490°C. Numerous contemporary studies highlight the importance of precise

microstructural control in lithium disilicate ceramics. For instance, specific firing protocols can influence translucency without significantly compromising flexural strength. The resulting microstructure, particularly the size and distribution of needle-shaped $LiAlSi_2O_6$ crystals, profoundly impacts both the optical and physical properties of the final restoration. Determining the optimal nucleation and crystallization temperatures fundamentally depends on the specific composition of the glass-ceramics system. These materials generally exhibit low-to-moderate mechanical properties when compared to natural enamel. Literature reports hardness values for various lithium disilicate formulations typically ranging from 5.3 GPa to 8.4 GPa (Huang, Zhang, et al., 2013), and 8.07 GPa (Zhang, Wang and Han, 2023), 6.88±0.39 for hardness and 98.9± 2.82GPa (Huang, Zhang, et al., 2013), 90 GPa (Zhang, Wang and Han, 2023) and 60.5 GPa (Ma et al., 2025) for elastic modulus. It is essential to compare these values with natural tooth structure to assess biomechanical compatibility. Human enamel exhibits an average hardness of approximately 3 to 5 GPa and an elastic modulus of 70 to 100 GPa, while the softer underlying dentin possesses a much lower hardness of around 0.7 GPa and an elastic modulus of 20 GPa (Chen and Liu, 2014; Zaytsev and Pan, 2014; Zhang et al., 2014; Niu et al., 2019; Zhao et al., 2022). The goal in restorative dentistry is not always maximum strength, but optimal compatibility. A higher elastic modulus in a restorative materials than the surrounding tooth structure can lead to a significant issue known as stress shielding where the restoration most of the biting force and shields the underlying natural tooth structure, potentially leading to secondary fractures or failure at the interface. The current challenge in improving Li-Al-Si glass ceramics for high-performance dental applications lies in the precise correlation between controlled heat treatment parameters and the resulting microstructure, mechanical strength, and surface quality. Therefore, this study aims to investigate the optimal temperature/time thermal profile of nucleation and crystallization in Li-Al-Si glass, using XRD phase analysis, to gain a comprehensive understanding of the phase assemblage and its relationship to improving mechanical properties (hardness and modulus of elasticity) and surface roughness, ensuring that the resulting material is more durable, effective, and safe for clinical applications.

2. MATERIALS AND METHODS

The material used in this study is glass within the LiO_2-Al_2O_3-SiO_2 (LAS) system with composition 10-8 wt% LiO_2, 10-5 wt% Al_2O_3, and 70-60 wt% SiO_2 with trace amounts of nucleating agents that are carefully selected to promote controlled crystallization of the desired phase. Rectangular samples of 14mm (width) x 12mm (thickness) x 18mm (height) were used for the assessment of the heat treatment effect on their microstructure and mechanical

properties. A total of eight heat-treated samples and one raw glass sample were prepared, with five measurements recorded for each sample for hardness, elastic modulus, and roughness. To investigate the ceramic process system (ceramming process) desirable glass sample heated treatment as showing the profiles brief in Table 1. After the final holding time, all samples were cooled to room temperature inside the furnace at a controlled cooling rate of 10°C/min to prevent thermal shocking and minimize the formation of undesired phases. As mentioned, these profiles were designed on several prior studies involving the DTA thermal analysis of glass-ceramics (Laczka et al., 2014), which closely equate to glass-ceramics in this study.

2.1. Heat treatment

The heat treatment profiles applied to the LAS glass samples were determined based on a comprehensive differential thermal analysis (DTA) of. Where they were toward following; first set was to investigate how holding time affect the nucleation stage of heat treatment which was at 520°C with 0-60min, as shown in Table 1. While the second set was designed to study the influence of increase gradually of crystallization temperature, initiate from 750°C and 900°C with 0-60min, as seen in Table 1. This set was aimed to achieve two objectives; first one is to investigate how nucleation process affect the crystallization process, second one is to optimize the impact of crystallization temperature with different a holding time.

Table 1. Heat treatment tailored by the examined samples.

Profile ID	Description	Nucleation	Crystallization	
		Stage I (520°C)	Stage II (750°C)	Stage III (900°C)
		Hold Time	Hold Time	Hold Time
Raw Glass	Amorphous	—	—	—
Profile 1	Nucleation Only	0 min	—	—
Profile 2	Extended Nucleation	60 min	—	—
Profile 3	Nucleation & Low Temp Crystal 1	0 min	0 min	—
Profile 4	Nucleation & Low Temp Crystal 2	60 min	0 min	—
Profile 5	Nucleation & Extended Low Temp Crystal	60 min	60 min	—
Profile 6	Multi-stage II	0 min	0 min	0 min
Profile 7	Multi-stage III	0 min	0 min	60 min
Profile 8	Optimized Multi-stage	60 min	0 min	60 min

After completing the final crystallization stage, all samples underwent a controlled cooling procedure by turning off the furnace power and allowing the samples to cool slowly within the furnace chamber to room temperature overnight. This controlled cooling ensures consistency and repeatability and prevents thermal shock that could induce micro-cracks.

2.2. X-ray diffraction (XRD)

In-situ high temperatures XRD measurements were carried out an AL-2700 series diffractometer (Dandong Aolong Radiative Instrument Group Co., Ltd.) equipped with CuKα radiation, wavelength λ=0.15418 nm operated using a current of 40 mA, a voltage 40 kV. The

XRD patterns were performed using a 2θ range of 10–80° and scan rate of 3° min^{-1}.

2.3. Surface roughness

A roughness tester manufacturing INSIZE (CODE: separable-type ISR-C300, Suzhou, China) was employed to estimate the surface roughness of the samples with a length of 2 mm. Next the samples were positioned on a stable board over the test to ensure accurate the measurement microgeometry of the surface. To detect the profile of the surface irregularities, four readings were recorded with difference sites for each sample, finally the mean values of these readings were calculated.

2.4. Elastic modulus

For prepare sample to be suitable for enhanced ultrasonic coupling. Grinding is carried out to minimize surface protuberances present on the cast ingots. This process employs abrasive SiC papers with successively finer particle sizes until an even surface is prepared for subsequent polishing. Hence, initially grinding was carried out with a nominal P120 grit, whereas final grinding was with P1200 grit. Diamond paste was employed to attain a 6μm surface finishing. The elastic modulus was calculated by measuring the ultrasound wave speed of glass-ceramics using pulse echo overlap method. The phase velocity (ultrasound wave speed) is determined solely from the density and the elastic properties of the material. It is calculated using the equation for the speed of ultrasonic waves, indicated by the Eq.1 (Hu and Wang, 2016; Hübschen, 2016).

$$V_s = \sqrt{\frac{E}{2\rho(1+\nu)}} \qquad (1)$$

Where; V_s Shear wave velocity, Ultrasound speed m/s, ρ Density of material, kg/m^3, E Elastic modulus, GPa, ν Poisson's ratio=0.25 for glass-ceramic (International Organization for Standardization, 2015).

2.5. Knoop Hardness (HK)

Specimens (18mm×14mm×12mm) of each heated treated ceramic were configured, grinded and polished using a SiC papers and diamond pastes. A digital instrument micro-hardness tester was employed to measure the hardness (HK) by Knoop's method using a long diagonal indenter to create an indentation on a material's surface. The hardness (HK) was carried out with a applied force (1.998kg.f) which is appropriate for glass-ceramics resulting in creates a rhombic pyramid elongated, making a long shallow indent ideal being suitable for brittle materials. To assert valid measurements, the contact surface of the tester was aligned with the sample platform. Meanwhile testing, the gap which is the sample surface and the indenter was modified to 5–12mm. The dwelling time of the indenter remained on the sample was 10 seconds,

according to ASTM E384−17 (ASTM Committee, 2016). The Knoop hardness for each specimen was calculated using Knoop Eq.2.

$$HK = \frac{P}{C\,L^2} \quad (2)$$

Where HK is the hardness, P is the applied load (kg.f), L is the length of the long diagonal in mm and C is a constant accounting for the indenter's geometry = 0.070279. The five multiple areas of each sample can be selected, to measure five readings and the mean of these readings was calculated.

2.6. Scanning Electrons Microscopy (SEM)

Scanning electron microscopy (SEM) (Inspect S50 manufactured by the FEI Company in the Netherlands) next to energy dispersive X-ray spectroscopy (EDS) was employed to inspect the surface morphology of glass and glass-ceramic samples. The monitoring operation was executed under a low accelerating voltage of 20 kV with low vacuum conditions (60 Pa) ,a short imaging duration (30 seconds) and a small spot size (3 nm), eliminating the demand for using chemical fixatives technique. To prepare the specimens, they were placed on two sides, and then the specimens were carried out gold coating by sputter coating equipment. The morphology of the designated glass-ceramics samples were subsequently investigated and compared.

3. RESULTS AND DISCUSSION

3.1. Ex-situ X- ray diffraction of LAS glass

The phase growth can be elucidated by X-ray diffraction (XRD) analysis providing evidence of the controlled crystallization process and could be immediately associated with the observed microstructural and mechanical properties. The XRD pattern of the raw glass exhibits an amorphous structure in which showing a broad hump centered around 2θ: 20-30°, confirming the characteristic long range structural disposition of the vitreous (glassy) state (Holand et al., 2006; Zheng et al., 2008; Huang, Zhang, et al., 2013; Deubener et al., 2018; Honma et al., 2022). The pattern for the sample treated at nucleation temperature (520°C for 60 minutes), profile 3, shows the constancy of this amorphous condition; however, the first of low-intensity and broad peaks emerged at low trace within range ~ 2θ:35°-45° indicates the initial formation of a lithium silicate (Li_2SiO_3) solid solution phase and lithium orthophosphate (Li_3PO_4) nuclei, as shown in Fig. 1.

The lithium orthophosphate (Li_3PO_4) phase plays role as a common nucleation agent in Li-Al-Si glass systems in which subsequently providing heterogeneous nucleation sites, confirming the performance of the low-temperature at 520°C. This may contribute to initiation of phase

separation without substantial crystal growth (Laczka, Cholewa-Kowalska and Laczka, 2014). In contrast, the patterns of the heated treated crystallized samples above 750°C, above profile 4, are dominated by sharp-edged and high-intensity diffraction peaks. The phases were identified a lithium aluminosilicate $LiAlSi_2O_6$ as main phase and a lithium disilicate $Li_2Si_2O_5$ as minor phase, with the most intense peaks corresponding to the (within range ~ 2θ:26°-29°) and (2θ:30°) crystallographic planes of lithium aluminosilicate and lithium disilicate, respectively, as depicted in Fig. 2. The intensity sharped of these peaks suggests a unique crystal structure and a high-degree of crystalline (Holand et al., 2006). The presence of these interlocking and high-degree crystalline phases, determined by XRD as depicted in Fig. 2, is the fundamental microstructural reason for the superior mechanical performance, involving hardness and elastic modulus in this study, observing in profile 4, 5, 6, 7 and 8 samples, therefore this is a well-established relationship in glass-ceramic system (Sun et al., 2021).

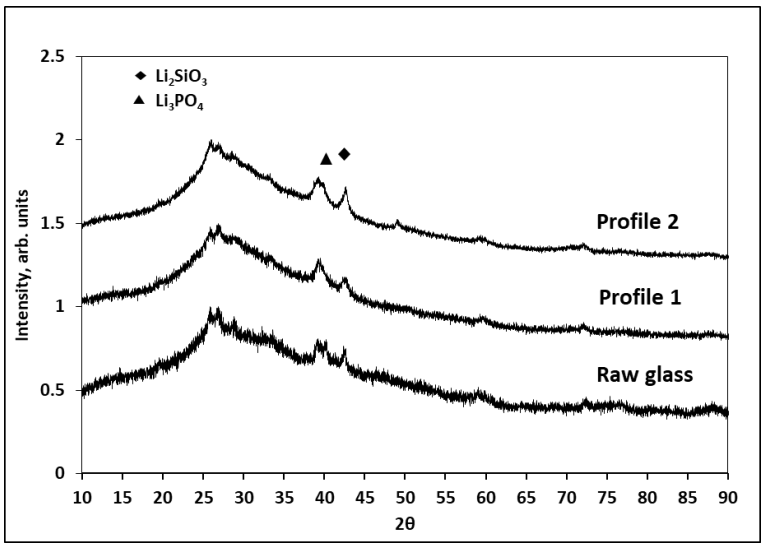

Fig. 1. XRD patterns of raw LAS glass and nucleated glass.

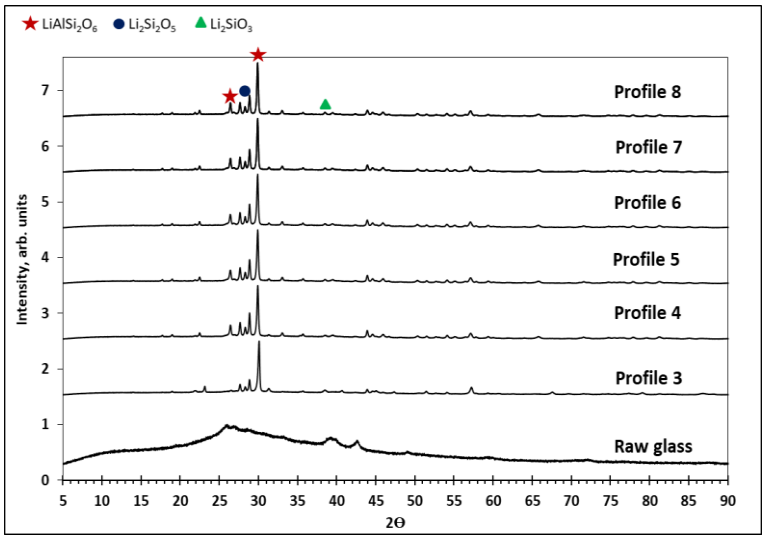

Fig. 2. XRD patterns of the heat treatment 520°C, 750°C and 900°C for different times.

3.2. Roughness surface properties including Ra and Rz

The inherent surface roughness of the LAS glass-ceramics is not a random topographic feature but a direct physical aspect of the underlying crystalline microstructure, as showing identified by XRD analysis. As above mentioned in XRD analysis that samples treated at profiles 1, 2 and 3 indicated only the initial formation of lithium phosphate nuclei within a predominant amorphous phase resulting in a relatively smooth but undulating surface. This topography arises from the nanoscale phase separation which precedes full crystallization, producing a slightly textured surface, characterizing the lowest recorded arithmetic mean roughness (Ra) of 0.34±0.04 μm and a minimum height (Rz) of 1.53±0.14 μm. In contrast, the low surface roughness (Ra, Rz) obtained in the profile 5 (750°C for 60 minutes) sample is a direct consequence of its crystalline characterizing by the low recorded arithmetic mean roughness (Ra) of 0.36±0.04 μm and a minimum height (Rz) of 1.78±0.12 μm. Although this (Ra) value is higher than the clinically recommended limit of 0.2 μm for minimizing bacterial adhesion, it represents the lowest roughness that could be achieved for unpolished surface via heat treatment process (Alhassan et al., 2022; Tuysuz, Demir and Yuzbasioglu, 2025), demonstrating the remarkable effect of the process of smoothing surface as a fundamental processing in preparing this material to receive a restoration for dental applications. XRD pattern for this condition asserts the predominant precipitation of lithium aluminosilicate $LiAlSi_2O_6$ and lithium disilicate $Li_2Si_2O_5$, phases recognized to form a densely interlocking microstructure and fine-grained as see in SEM images. This homogeneous distribution of fine crystals minimizes the peak-to-valley height (Rz) via preventing the formation of prominent crystalline or deep crystal valleys, resulting in a smooth surface. In contrast, the elevated roughness of the profile 8 sample appears and could be explained by its XRD results as shown in Fig. 3. XRD pattern suggests not only lithium aluminosilicate $LiAlSi_2O_6$ but also the potential formation of additional such as the remained metasilicate phase, often rough, crystalline phases, as seen in XRD analysis. This multi-phase microstructure as in profile 5, with crystals of differing sizes and growth habits, creates a more pronounced and irregular surface relief, increasing both Ra and Rz. Therefore, XRD provides the fundamental reason for the observed roughness: the presence, identity, and proportion of crystalline phases dictate the microstructural landscape that is replicated on the surface.

3.3. Mechanical properties including the elastic modulus, hardness

The measured mechanical properties, namely the Knoops hardness (HK) and elastic modulus (E), exhibit a direct and predictable correlation with the crystalline phase growth identified by XRD, confirming the principle that the microstructure controls mechanical performance. The

synergistic relationship between surface roughness, mechanical properties (hardness and elastic modulus), and crystalline phase content, as revealed by XRD, defines the overall performance of the material. The raw amorphous glass exhibited the lowest values for both hardness (HK) and elastic modulus (E) by 5.4 GPa and 80.76 GPa respectively, due to disordered crystalline lattice planes (presence of structural disorder) results in a poor ability to form and move dislocations under stress/load, which are the primary mechanism for plastic flow in crystals (Idrissi, Carrez and Cordier, 2022). This state is confirmed by the broad hum in its XRD pattern indicating amorphous solids. It is important to contrast these findings with the natural enamel exhibits an elastic modulus of 70-100 GPa, in addition to the dentin of 18-20 GPa (Chen and Liu, 2014; Zaytsev and Pan, 2014; Zhang et al., 2014; Niu et al., 2019; Zhao et al., 2022). While the high elastic modulus of the profile 5 sample 96.33 GPa indicates superior stiffness and fracture resistance, this significant mechanical mismatch with the dentin could potentially lead to stress shielding or undesirable stress concentrations in the tooth structure, a critical consideration for long-term clinical success. The XRD pattern for the optimal profile 5 condition (750°C/60min), that lithium aluminosilicate phase $LiAlSi_2O_6$ dominates the crystalline phases, is key to understanding its superior performance. The nature of interlocking and fine-grained of this phase, as confirmed by XRD, simultaneously performs two critical goals; first, to produce hard and durable crystal boundaries that intrinsically resists deformation (high Knoops hardness) and elastic strain (high elastic modulus). Second, this is very fine-grained microstructure demonstrates as an inherent textured surface with low Ra and Rz values (Temmler et al., 2020). This is mechanically critical because, according to mechanics, surface flaws act as stress concentrators. The low Rz value of this sample signifies the absence of severe fracture that initiating flaws (Arsecularatne, Dingeldein and Hoffman, 2015). Thus, the lithium aluminosilicate phase $LiAlSi_2O_6$ identified by XRD is responsible for both a high intrinsic resistance to deformation and a flaw-tolerant surface, resulting in the best mechanical performance. In contrast, the below level properties of the profile 8 sample are a direct consequence of the microstructural degradation from its XRD pattern. The formation of crystals or secondary phase results in a rougher surface (high Rz) filled with deep valleys that act as strong stress concentrators exhibiting the material to fracture. However, the crystallinity may still accord suitable high hardness; the severe surface flaws fairly restrict the effective strength. Meanwhile, the profile 2 and 3 samples lack the extensive crystalline reinforcement shown by its XRD pattern, resulting in lower intrinsic hardness and modulus, despite its relatively smoother surface. Hence, the XRD analysis conclusively shows that the lithium aluminosilicate phase $LiAlSi_2O_6$ formed above 750°C is uniquely optimal for developing a microstructure in

particular profile 5 that delivers the ideal combination of high intrinsic mechanical properties including hardness, elastic modulus by values 7.663 GPa and 96.233 GPa respectively, as shown in Fig. 4 and 5 and a low stress concentration surface topography by values Ra of 0.36±0.04 µm and Rz of 1.78±0.12 µm, as shown in Fig. 3.

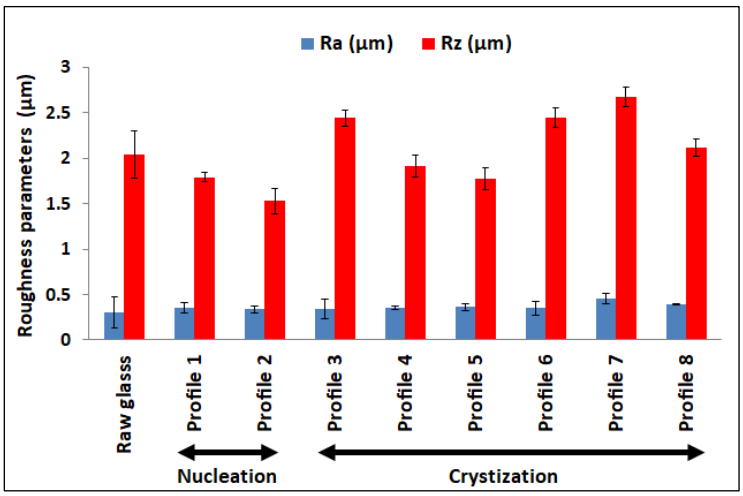

Fig. 3. Surface roughness parameters of the heat treatment 520°C, 750°C and 900°C for different times.

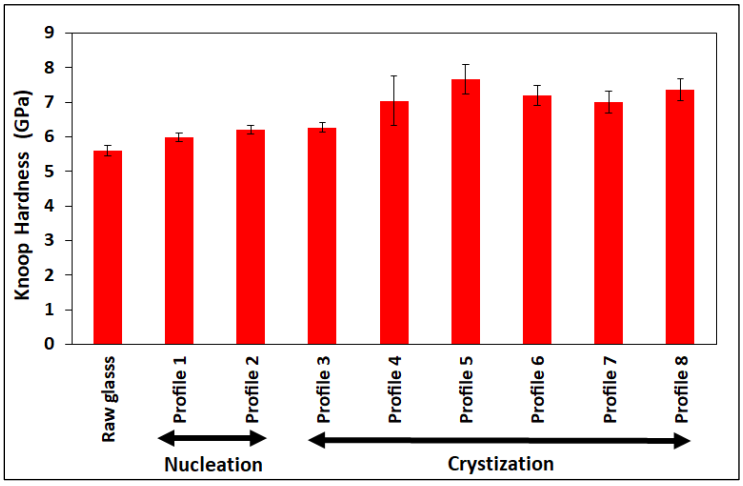

Fig. 4. Knoop hardness of the heat treatment 520°C, 750°C and 900°C for different times

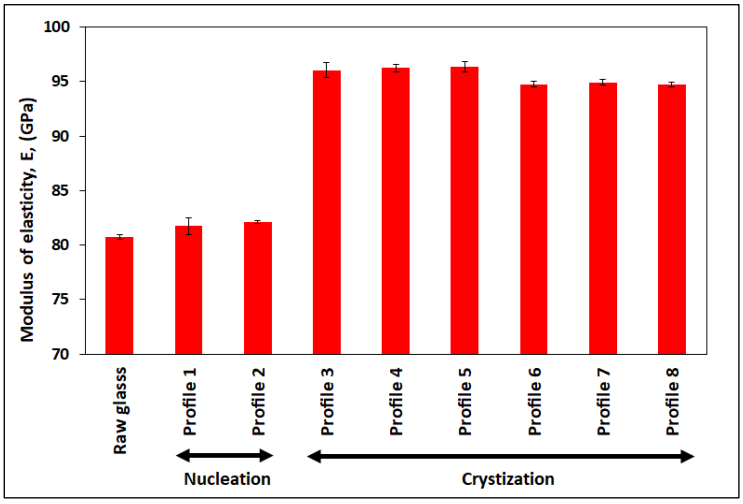

Fig. 5. Modulus of elastic of the heat treatment 520°C, 750°C and 900°C for different times.

Comparing the results of this study with previously published findings on the properties of lithium-alumino-silicate (LAS) glass-ceramics reveals a clear trend in the overall mechanical properties. Hardness values reported in previous studies ranged from 5.3 to 8.4 GPa, closely matching the hardness measured in this study for untreated samples (5.4 GPa). This suggests that the raw glass structure exhibits properties similar to those reported in the literature. This is convergence is typically associated with the proportion of residual glass and the absence of a dominant crystalline phase, as confirmed by the broad XRD patterns of the amorphous state. Regarding the modulus of elasticity, previous studies have reported a wide range of values between 50 and 98.9 GPa, with average values close to 86.8 GPa for LAS systems treated at similar temperatures in (Huang, Zhang, et al., 2013; Zhang, Wang and Han, 2023; Ma et al., 2025). The modulus of elasticity measured in this study (80.76 GPa) falls within this range, confirming that the crystallization mechanism and crystalline phase growth follow trends documented in the literature, particularly during the transition from a glassy to a semi-crystalline state. Previous studies also support the direct relationship between the growth of the $Li_2Si_2O_5$ or $LiAlSi_2O_6$ crystalline phase and improved mechanical properties such as hardness and modulus of elasticity. The interlocking growth of fine grains leads to increased resistance to deformation and elastic strain (Arnon et al., 2022). This aligns with the findings of the optimal sample (profile 5), which exhibited the highest mechanical values in this study by 7.663 GPa for hardness and 96.233 GPa for modulus of elasticity. These values are very similar to those reported in studies using comparable heat treatment schedules (Huang, Cao, et al., 2013). Conversely, the literature has documented that the transition to coarse or heterogeneous secondary phases leads to a decline in mechanical performance due to increased surface roughness and the emergence of stress concentrations (Elsherbini et al., 2025; Wally et al., 2025). This aligns with the findings for the profile 8 sample in this study, where the deterioration of the crystal structure resulted in an increased Rz value and consequently a significant decrease in toughness, despite the hardness remaining within acceptable limits. Thus, a comparison of the current results with previous studies demonstrates that the microevolution induced by heat treatment especially under optimal conditions at 750 °C that is consistent with established scientific trends and leads to an optimal combination of mechanical properties and surface homogeneity.

3.4. SEM Characterization nucleated and crystallized samples

The SEM microstructural analysis provides a vital visual confirmation of the crystalline phase growth identified by XRD, establishing an association between qualitative phase identification and topography surface in addition to detect material composition. The featureless observed in

the SEM image of the amorphous raw glass corresponds perfectly with the broad hump seen in its XRD pattern, both consistent with the absence of long range heat treatment. The critical role of the profile 2, the nucleation stage, is revealed under SEM as a fine-scale phase separation and uniform and the emergence of nanometric crystallites that generally small-scale to produce sharp XRD peaks, however, seen as a texturing of the glassy matrix as shown in Fig. 6-a, and b. In addition, SEM is detecting the initial microstructural changes that precede detectable long range crystal formation.

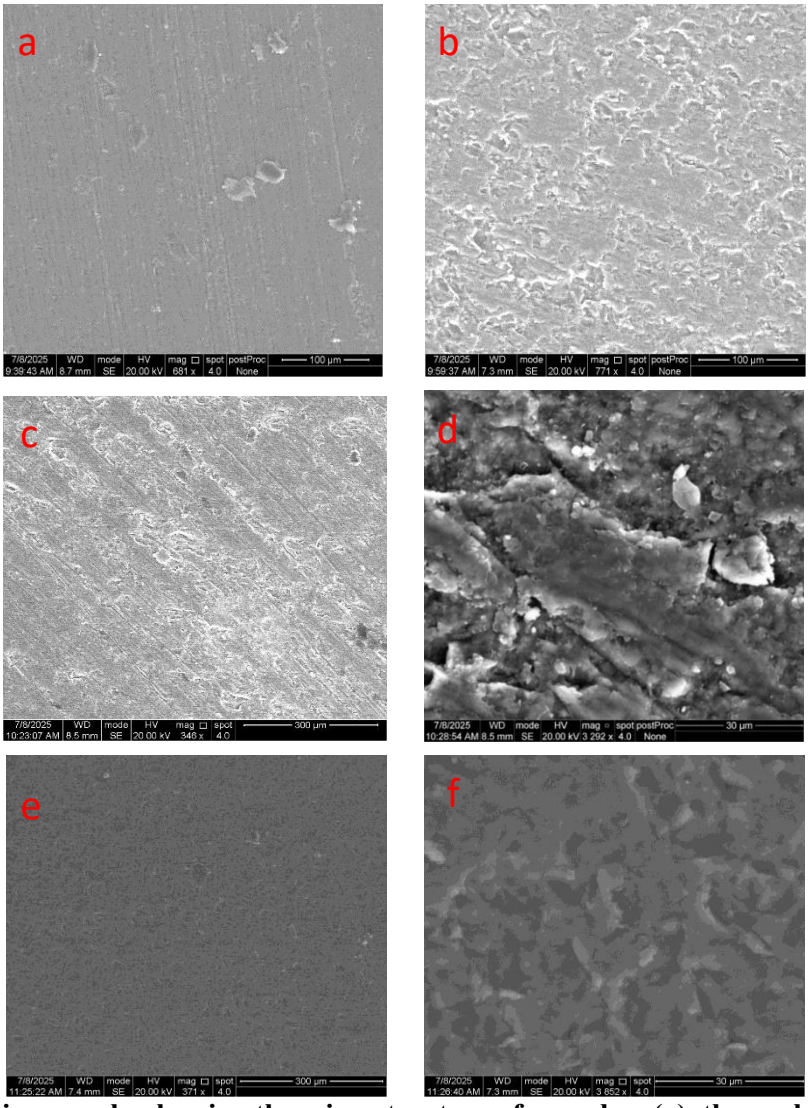

Fig. 6. SEM micrographs showing the microstructure of raw glass (a), the nucleated glass (b), the sample at 520°C, and subsequently heat treated at 750°C (c and d) and the sample at 520°C, and subsequently heat treated at 900°C.

As for the optimal treatment profile 5 sample, XRD pattern confirmed the dominant presence of the Lithium aluminosilicate ($LiAlSi_2O_6$) phase and the secondary phase is lithium disilicate ($Li_2Si_2O_5$). The SEM micrograph reveals a uniform and dense interlocking microstructure of fine, needle like crystals for $LiAlSi_2O_6$ and rod-like crystals for $Li_2Si_2O_5$, as shown in Fig. 6-c, d, e, and f. This fine-grained morphology of $LiAlSi_2O_6$ is a feature of effective nucleation and

controlled crystal growth, distinctly explaining the superior mechanical properties and low surface roughness. Furthermore, the SEM analysis of the profile 8 (900°C/60min) sample provides the microstructural reason for its low mechanical performance compared to profile 5 sample. XRD confirmed crystallization; the SEM image likely shows excessive crystal growth, leading to a coarse-grained structure with large, irregularly shaped crystals and potential micro-porosity at grain boundaries.

4. CONCLUSION

The superior properties are an acceptable outcome of interlocking microstructure of the Lithium aluminosilicate ($LiAlSi_2O_6$) as major phase dominating this kind of glass-ceramics, in addition the lithium disilicate ($Li_2Si_2O_5$), minor phase, as identified by XRD analysis and visually confirmed by SEM imaging.

A heat treatment of the profile 5 (750°C for 60 minutes) was established as the optimal heating for developing high-performance of this kind of dental LAS glass-ceramics yielding the best combination of mechanical and roughness surface properties.

Treatment at 520°C plays role only initiated nucleation, subsequently incomplete crystallization, however is the best optimization temperature as a nucleation temperature for a while (60min) instead of zero temperature. Moreover, treatment at 900°C generally led to uncontrolled crystal growth and rough microstructure, increasing surface roughness and low mechanical performance to a certain degree.

This optimal microstructure simultaneously resulted in the higher knoops hardness and elastic modulus, indicating superior intrinsic strength. However, future work must evaluate the clinical trade-off. While high modulus is desirable for strength, its potential for inducing stress shielding compared to natural dentin requires careful consideration in dental restorations.

This material is accompanied by an inherently smooth surface characterizing by the lowest values of average roughness (Ra) and maximum peak-to-valley height (Rz). However, the recorded roughness values exceeded the clinically recommended limit of 0.2 μm. This research demonstrates that careful calibration of the thermal cycle is not only critical for achieving desired mechanical properties, yet the polishing as post-processing is necessity for dental applications.

ACKNOWLEDGEMENTS

The authors thank to Nanotechnology and advanced material research Unit in University of kufa (Dr. Abbas Ali Diwan and Dr. Muthanna Hassan Hadi) where the XRD experiments were completed. The authors thank to Dr Ahmed Al-antaki (Faculty of Science - University of Kufa)

due to his contribution to achieve SEM images and Dr Maytham Saad Ali (Faculty of Engineering - University of Kufa) due to his contribution to using and measuring surface roughness.

5. REFERENCES

Abd-Elaziem, W. et al. (2024) 'Titanium-Based alloys and composites for orthopedic implants Applications: A comprehensive review', Materials and Design. Elsevier Ltd, 241(December 2023), p. 112850. doi: 10.1016/j.matdes.2024.112850.

Abdulkadhim, Z. G. (2014) 'Influence calcium carbonate nano-particles CaCO3 on mechanical properties for NR compound', International Journal of Mechanical and Mechatronics Engineering, pp. 114–117.

Adolfsson, E. and Shen, J. Z. (2014) 'Defect Minimization in Prosthetic Ceramics', in Advanced Ceramics for Dentistry. Elsevier Inc., pp. 359–373. doi: 10.1016/B978-0-12-394619-5.00017-1.

Al-hadrayi, Z. M. R. and Khaleel, H. H. (2025) 'MODELING AND EVALUATION OF VIBRATIONAL BEHAVIOR IN FUNCTIONALLY GRADED CERAMIC- METAL COMPOSITE BEAMS', Kufa Journal of Engineering, 16(2), pp. 35–57. doi: https://doi.org/10.30572/2018/KJE/160203.

Alhassan, M. et al. (2022) 'Effect of Different Surface Treatments on the Surface Roughness and Gloss of Resin-Modified CAD/CAM Ceramics', Applied Sciences, 12(23), p. 11972. doi: https://doi.org/10.3390/app122311972.

Arnon, K. et al. (2022) 'Phase Formation, Mechanical Strength, and Bioactive Properties of Lithium Disilicate Glass–Ceramics with Different Al2O3 Contents', Materials, 15, p. 8283.

Arsecularatne, J. A., Dingeldein, J. P. and Hoffman, M. (2015) 'An in vitro study of the wear mechanism of a leucite glass dental ceramic', Biosurface and Biotribology. Elsevier, 1(1), pp. 50–61.

ASTM Committee (2016) 'Standard test method for microindentation hardness of materials', West Conshohocken, PA, USA, 384, p. 399.

Chen, H. and Liu, Y. (2014) 'Chapter 2. Teeth', in Shen, J. Z. and Kosmač, T. (eds) Advanced Ceramics for Dentistry. Elsevier Inc., pp. 5–21.

Deubener, J. et al. (2018) 'Updated definition of glass-ceramics', Journal of Non-Crystalline Solids, 501(February), pp. 3–10. doi: 10.1016/j.jnoncrysol.2018.01.033.

El-Meliegy, E. and Noort, R. van (2012) Glasses and Glass Ceramics for Medical Applications. New York: Springer Science+Business Media, LLC. doi: 10.1007/978-1-4614-1228-1.

Elsherbini, A. et al. (2025) 'Mechanical Performance and Surface Roughness of Lithium Disilicate and Zirconia-Reinforced Lithium Silicate Ceramics Before and After Exposure to Acidic Challenge', Dentistry Journal, 13(117), pp. 1–16. doi: https://doi.org/10.3390/dj13030117.

Fatlawi, A. Al, Jármai, K. and Kovács, G. (2021) 'Optimal design of a lightweight composite sandwich plate used for airplane containers', Structural Engineering and Mechanics, 78(5), pp. 611–622. doi: https://doi.org/10.12989/sem.2021.78.5.611.

Fu, L., Engqvist, H. and Xia, W. (2020) 'Glass–Ceramics in Dentistry : A Review', Materials, 13(5), p. 1049.

Holand, W. et al. (2006) 'Studies of crystal phase formations in high-strength lithium disilicate glass–ceramics', Journal of Non-Crystalline Solids, 352, pp. 4041–4050.

Honma, T. et al. (2022) 'Unique properties and potential of glass-ceramics', Journal of the Ceramic Society of Japan, 130(8), pp. 545–551. doi: https://doi.org/10.2109/jcersj2.22037.

Hu, E. and Wang, W. (2016) 'The Elastic Constants Measurement of Metal Alloy by Using Ultrasonic Nondestructive Method at Different Temperature', Mathematical Problems in Engineering, 2016(ID 6762076, 7 pages). doi: http://dx.doi.org/10.1155/2016/6762076.

Huang, S., Zhang, B., et al. (2013) 'Crystalline phase formation, microstructure and mechanical properties of a lithium disilicate glass–ceramic', Journal of Materials Science, 48(1), pp. 251–257.

Huang, S., Cao, P., et al. (2013) 'Fabrication of a high-strength lithium disilicate glass-ceramic in a complex glass system', Journal of Asian Ceramic Societies, 1(1), pp. 46–52.

Hübschen, G. (2016) 'Ultrasonic techniques for materials characterization', in Materials Characterization Using Nondestructive Evaluation (NDE) Methods, pp. 177–224. doi: 10.1016/B978-0-08-100040-3.00007-9.

Idrissi, H., Carrez, P. and Cordier, P. (2022) 'On amorphization as a deformation mechanism under high stresses', Current Opinion in Solid State and Materials Science. doi: 10.1016/j.cossms.2021.100976.

International Organization for Standardization (2015) International Standard ISO 6872: Dentistry - Ceramic materials. 4th edn. Geneva: ISO.

Jasim, Z. M. and Abdulsamad, H. J. (2025) 'INVESTIGATION OF FREE VIBRATION BEHAVIOR FOR COMPOSITE SANDWICH BEAMS WITH A COMPOSITE HONEYCOMB CORE', Kufa Journal of Engineering, 16(1), pp. 177–199. doi: https://doi.org/10.30572/2018/KJE/160111.

Jweeg, M. J. and Al-Jlaihawi, Z. G. (2021) 'Characterization of Natural Rubber (NR), Polybutadiene Rubber (BR) and Styrene-Butadiene Rubber (SBR) Blends Cured in a Vulcanization System', Materials Science Forum, 1039, pp. 51–64. doi: https://doi.org/10.4028/www.scientific.net/MSF.1039.51.

Kordatos, E., Abdulkadhim, Z. and Feteira, A. E. (2017) 'Non-destructive thermo-mechanical behavior assessment of glass- ceramics for dental applications', in Proc. SPIE 10214, Thermosense: Thermal Infrared Applications XXXIX. Anaheim, California, United States. doi: doi: 10.1117/12.2262580.

Laczka, K., Cholewa-Kowalska, K. and Laczka, M. B. (2014) 'Thermal and spectroscopic characterization of glasses and glass–ceramics of Li2O–Al2O3–SiO2 (LAS) system', Journal of Molecular Structure journal, 1068, pp. 275–282.

Laczka, M. et al. (2014) 'Mechanical Properties of a Lithium Disilicate Strengthened Lithium Aluminosilicate Glass-Ceramic', Journal of the American Ceramic Society, 97(2), pp. 361–364.

Ma, J. et al. (2025) 'Journal of Materials Science & Technology β -spodumene-doped lithium disilicate glass-ceramics via additive manufacturing for dental applications', Journal of Materials Science & Technology. Elsevier Ltd, 247, pp. 289–301. doi: 10.1016/j.jmst.2025.04.082.

Niu, H. et al. (2019) 'Journal of the Mechanical Behavior of Biomedical Materials Elastic properties measurement of human enamel based on resonant ultrasound spectroscopy', Journal of the Mechanical Behavior of Biomedical Materials. Elsevier Ltd, 89(August 2018), pp. 48–53. doi: 10.1016/j.jmbbm.2018.09.014.

Pershin, V. et al. (2018) 'A Graphene Masterbatch for Modification of Frost-Resistant Plastic Lubricants', AIP Conference Proceedings, 020016. doi: https://doi.org/10.1063/1.5079347.

Remote, U. et al. (2019) 'Simulation of graphene-containing viscous fluid motion in the gap between static and rotating discs Simulation of graphene-containing viscous fluid motion in the gap between static and rotating discs', IOP Conf. Series: Journal of Physics, 1278. doi: doi:10.1088/1742-6596/1278/1/012025.

Sun, Y. et al. (2021) 'Effects of heat-treatment temperature and holding time on the microstructure and mechanical properties of lithium disilicate glass-ceramics', Journal of Non-Crystalline Solids. Elsevier B.V., 553(October 2020), p. 120502. doi: 10.1016/j.jnoncrysol.2020.120502.

Temmler, A. et al. (2020) 'Influence of laser polishing on surface roughness and microstructural properties of the remelted surface boundary layer of tool steel H11', Materials and Design. The Author(s), 192, p. 108689. doi: 10.1016/j.matdes.2020.108689.

Tuysuz, C. C., Demir, N. and Yuzbasioglu, E. (2025) 'Does Repolishing Affect the Gloss and Roughness of Lithium Disilicate and Monolithic Zirconia Ceramics?', Applied Sciences, 15, p. 4622. doi: https://doi.org/10.3390/ app15094622.

W. Höland and G. H. Beall (2012) Glass-Ceramic Technology. Second Ed. New Jersey: The American Ceramic Society.

Wally, Z. J. et al. (2025) 'Effects of incorporating magnesium oxide and zirconium dioxide nanoparticles in acrylic resin denture base material : a comparative study', Frontiers in Dental Medicine, 6, p. 1667644. doi: 10.3389/fdmed.2025.1667644.

Zainy, H. Z. et al. (2025) 'THEORETICAL AND EXPERIMENTAL INVESTIGATION OF CRITICAL BUCKLING LOAD OF COMBINED COLUMNS', Kufa Journal of Engineering, 16(1), pp. 344–360.

Zaytsev, D. and Pan, P. (2014) 'Deformation behavior of human enamel and dentin – enamel junction under compression', Materials Science and Engineering C, 34, pp. 15–21. doi: https://doi.org/10.1016/j.msec.2013.10.009.

Zhang, X., Wang, J. and Han, J. (2023) 'Crystallization kinetics, structural and mechanical properties of transparent lithium aluminosilicate glass-ceramics', Journal of Non-Crystalline Solids. Elsevier B.V., 603(December 2022), p. 122113. doi: 10.1016/j.jnoncrysol.2022.122113.

Zhang, Y. R. et al. (2014) 'Review of research on the mechanical properties of the human tooth', International Journal of Oral Science, 6(2), pp. 61–69.

Zhao, H. et al. (2022) 'Review Natural tooth enamel and its analogs', Cell Reports Physical Science. The Author(s), 3(7), p. 100945. doi: 10.1016/j.xcrp.2022.100945.

Zheng, X. et al. (2008) 'Effects of P2O5 and heat treatment on crystallization and microstructure in lithium disilicate glass ceramics', Acta Materialia, 56, pp. 549–558.

Zhou, Z. et al. (2022) 'Influences of Al2O3 content on crystallization and physical properties of LAS glass-ceramics prepared from spodumene', Journal of Non-Crystalline Solids. Elsevier B.V., 576(November 2021), p. 121256. doi: 10.1016/j.jnoncrysol.2021.121256.